0026-895X/11/8005-930–942$25.00
MOLECULAR PHARMACOLOGY
Copyright © 2011 The American Society for Pharmacology and Experimental Therapeutics
Mol Pharmacol 80:930–942, 2011

Vol. 80, No. 5
71621/3726651
Printed in U.S.A.

Strong Activation of *ether-à-go-go*-Related Gene 1 K^+ Channel Isoforms by NS1643 in Human Embryonic Kidney 293 and Chinese Hamster Ovary Cells

Anna M. Schuster, Günter Glassmeier, and Christiane K. Bauer

Institute of Cellular and Integrative Physiology, University Medical Center Hamburg-Eppendorf (UKE), Hamburg, Germany

Received February 6, 2011; accepted August 19, 2011

ABSTRACT

Two different mechanisms leading to increased current have been described for the small-molecule human *ether-à-go-go*-related gene (herg) activator NS1643 [1,3-bis-(2-hydroxy-5-trifluoromethylphenyl)-urea]. On herg1a channels expressed in *Xenopus laevis* oocytes, it mainly acts via attenuation of inactivation and for rat (r) erg1b channels expressed in human embryonic kidney (HEK)-293 cells, it strongly shifts the activation curve to the left. We now investigated the NS1643 effects on erg1b channels in more detail and performed comparative experiments with rat and human erg1a in different expression systems. Significant differences were observed between expression systems, but not between the rat and human isoform. In HEK-293 or Chinese hamster ovary (CHO) cells, activation of rat erg1b channels occurred in a dose-dependent manner with a maximum current increase of 300% obtained with 10 μM NS1643. In contrast, the NS1643-induced strong leftward shift in the voltage dependence of activation further increased with higher drug concentration, needed more time to develop, and exhibited use dependence. Coexpression of KCNE1 or KCNE2 did not attenuate this NS1643 effect on erg1 channel activation and did thus not mimic the lower drug potency on this parameter observed in oocytes. NS1643 (10 μM) slowed erg1b channel deactivation and recovery from inactivation without significant changes in activation and inactivation kinetics. With the exception of accelerated activation, NS1643 affected erg1a channels similarly, but the effect was less pronounced than in erg1b or erg1a/1b channels. It is noteworthy that rerg1b and herg1a inactivation estimated from fully activated current voltage relationships were unaltered in the continued presence of 10 μM NS1643 in the mammalian expression systems, indicating qualitative differences from NS1643 effects in *X. laevis* oocytes.

Introduction

The cardiac action potential controls the contraction of the heart by a very accurate regulated process that is mediated by changes in membrane permeability to specific ions. Voltage-gated potassium channels are of crucial importance for the action potential duration and the refractory period. In particular, the slow (I_{Ks}) and the rapid (I_{Kr}) delayed rectifier play an important role in the repolarization of cardiac muscle cells (Sanguinetti and Jurkiewicz, 1990). The pore-forming component of the I_{Kr} channel is encoded by the human *ether-à-go-go*-related gene (herg) (Warmke and Ganetzky, 1994; Sanguinetti et al., 1995; Trudeau et al., 1995). The typical gating of erg channels, including voltage-dependent fast inactivation and recovery from inactivation as well as slow deactivation, supports the plateau phase and explains the high impact during the repolarization of the cardiac action potential.

In addition to the classic full-length herg (herg1a) channel, the N-terminal splice variant herg1b was identified in the heart (Lees-Miller et al., 1997; London et al., 1997) and was shown to contribute to native heteromeric erg1a/1b channels in the heart (Jones et al., 2004). erg1b lacks a wide part of the N terminus of herg1a (amino acids 1–376), including the PAS [periodicity/aryl hydrocarbon receptor nuclear translocator/single-minded (Per-ARNT-Sim)] or EAG domain, and exhibits instead a much shorter unique N-terminal sequence of 36 amino acids. Because the EAG domain is crucial for the slow deactivation of erg channels (Schönherr and Heinemann, 1996), erg1b shows much faster deactivation kinetics than erg1a (Lees-Miller et al., 1997; London et al., 1997). The extent and significance of contributions of β-subunits such as KCNE1 or KCNE2 to

Article, publication date, and citation information can be found at http://molpharm.aspetjournals.org.
doi:10.1124/mol.111.071621.

ABBREVIATIONS: herg, human *ether-à-go-go*-related gene; HEK, human embryonic kidney; rerg, rat *ether-à-go-go*-related gene; CHO, Chinese hamster ovary; EGFP, enhanced green fluorescent protein; NS1643, 1,3-bis-(2-hydroxy-5-trifluoromethyl-phenyl)-urea; E-4031, *N*-[4-[[1-[2-(6-methyl-2-pyridinyl)ethyl]-4-piperidinyl]carbonyl]phenyl]methanesulfonamide dihydrochloride; KCNE, voltage-gated potassium channel, Isk-related family; CA-105574, 3-nitro-*N*-(4-phenoxyphenyl) benzamide.

the native I_{Kr} conducting channels are still a matter of investigation (Weerapura et al., 2002).

In addition to their cardiac expression, erg1a and erg1b subunits are coexpressed in many excitable tissues, including a number of different smooth muscle preparations as well as several regions of the central nervous system, where erg2 or erg3 channel subunits also might be coexpressed. In these tissues, erg channels often modulate excitability by contributing to the maintenance of the resting membrane potential (for review, see Schwarz and Bauer, 2004).

In the human heart, decreased function of I_{Kr} either by genetic mutations or more commonly by pharmacological block of erg channels can induce a long QT syndrome type 2. Reduced repolarizing currents result in a prolongation of the ventricular action potential, which increases the risk for life-threatening torsades de pointes arrhythmia and ventricular fibrillation. Therefore, unintended drug-induced block of erg channels presents a significant clinical and economical challenge in pharmacotherapy (Fermini and Fossa, 2003).

The induction of increased opening of erg channels and thus the acceleration of cardiac repolarization and shortening of action potential duration could present a novel antiarrhythmic principle (Grunnet et al., 2008). Consequently, an effort was made to develop compounds with herg channel-activating properties. In the last few years, several herg activators acting with different mechanisms have been identified (for review, see Li and Dong, 2010). The compound 1,3-bis-(2-hydroxy-5-trifluoromethyl-phenyl)-urea (NS1643) activates erg1 channels heterologously expressed in *Xenopus laevis* oocytes (Casis et al., 2006; Hansen et al., 2006; Xu et al., 2008) as well as the native I_{Kr} (Hansen et al., 2006; Diness et al., 2008). In animal studies, NS1643 has already been shown to provide antiarrhythmic properties (Diness et al., 2008; Killeen et al., 2008), but proarrhythmic effects have also been observed (Diness et al., 2008; Lu et al., 2008).

Reduced inactivation was described as the main mechanism of herg1a channel activation by NS1643 (Casis et al., 2006; Hansen et al., 2006; Xu et al., 2008). As we reported earlier, NS1643 exhibited a much stronger effect and a different mechanism of activation on rat erg1b (rerg1b) channels expressed in human embryonic kidney (HEK)-293 cells, where a strong shift in the voltage dependence of activation to more negative potentials was observed (Mewe et al., 2008). We have now extended our analysis and performed further experiments to investigate the pronounced activation of rerg1b channels by NS1643 in a mammalian expression system in more detail. In addition, we investigated whether reported discrepancies resulted from the use of different splice variants, different species or different expression systems. We found that the strongest effects of NS1643 on erg1b channels concerned the voltage dependence of activation and the deactivation kinetics, and our results show that the activation by NS1643 is indeed somewhat more pronounced for erg1b than for erg1a channels. Our data also suggest that the mechanism of erg1 channel activation by NS1643 depends on the expression system, because erg1a and erg1b inactivation remained unaltered in mammalian cells, which is in sharp contrast to the main mechanism of herg channel activation by NS1643 in *X. laevis* oocytes.

Materials and Methods

Cell Culture

HEK-293 cells, Chinese hamster ovary (CHO) cells, and CHO cells stably transfected with herg1a were cultured in Dulbecco's modified Eagle's medium (Invitrogen GmbH, Karlsruhe, Germany) supplemented with 1% penicillin-streptomycin-glutamine (Invitrogen) and 10% fetal calf serum (Biother, Kelkheim, Germany) at 37°C in a humidified incubator (95% air, 5% CO_2). The culture medium was changed every 2 to 3 days, and the cells were passaged when they reached confluence.

X. laevis Oocytes

X. laevis oocytes were collected under anesthesia (1.2 g/l tricaine), and the follicular tissue was removed by collagenase A (Roche, Basel, Switzerland). Before and after injection of cRNA, oocytes were kept at 18°C in Barth medium consisting of 88 mM NaCl, 3 mM KCl, 2.4 mM $NaHCO_3$, 0.82 mM $MgSO_4$, 0.3 mM $Ca(NO_3)_2$, 0.41 mM $CaCl_2$, and 15 mM Tris; pH adjusted to 7.4 with NaOH, supplemented with 50 mg/l gentamicin.

Heterologous Expression

Microinjection. HEK-293 cells were plated on glass coverslips coated with poly-D-lysine (Sigma-Aldrich, Deisenhofen, Germany) in 35-mm plastic culture dishes (NUNC, Wiesbaden, Germany) and microinjected with a Transjector 5246 (Eppendorf, Hamburg, Germany) with cDNA encoding either rat erg1b [rerg1b; 30 ng/μl (Hirdes et al., 2005)] or rat erg1a [rerg1a; 10 ng/μl (Bauer et al., 1998)] cloned into the pcDNA3 vector (Invitrogen). To allow detection of successfully expressing HEK-293 cells, EGFP-N1 (10 ng/μl; Clontech, Heidelberg, Germany) was coexpressed. Electrophysiological experiments were performed 8 to 24 h after injection. *X. laevis* oocytes were injected with cRNA encoding either rerg1a or herg1a using a Nanoliter 2000 microinjector (World Precision Instruments, Berlin, Germany). Oocytes were used for experiments 3 to 4 days after injection.

Transfection. HEK-293 or CHO cells plated onto poly-D-lysine-coated coverslips in 35-mm culture dishes were transfected with the relevant cDNA using LipofectAMINE 2000 reagent (Invitrogen, Karlsruhe, Germany) according to the manufacturer's instructions. For separate expression of rerg1a and rerg1b channels, cDNA encoding rerg1a (1 ng/μl) or rerg1b (1.8 ng/μl) was applied together with cDNA encoding EGFP-N1 (0.8 ng/μl; Clontech). Only for coexpression experiments of rerg1a together with rerg1b, rerg1a with C-terminally tagged EGFP [1 ng/μl (Kirchberger et al., 2006)] and rerg1b with C-terminally tagged DsRed [1 ng/μl (Kirchberger et al., 2006)] were used to enable identification of cells expressing both rerg1 subunits. In another set of experiments, rat KCNE1 (5.4 up to 10.8 ng/μl; GenBank Accession no. NM_012973) or KCNE2 (5.4 ng/μl up to 18 ng/μl; GenBank Accession no AF071003) was coexpressed together with rat erg1a or erg1b. Experiments were performed 8 to 48 h after transfection.

Electrophysiology. Membrane currents of erg1 channel expressing HEK-293 or CHO cells were recorded in the conventional whole-cell configuration of the patch-clamp technique. If NS1643 was applied during an experiment, cells were continuously superfused with external solution throughout the experiment. Patch pipettes were made from 1.5-mm diameter borosilicate glass capillaries with resistances of 2 to 4 MΩ. Data were low-pass filtered at 3 kHz and compensated for both fast and slow capacity transients before the pulse protocols. The access resistance ranged from 3 to 12 MΩ, and series resistance compensation was as high as possible (60–85%). Data were not corrected for the liquid junction potential error (~4 mV). An EPC-9 patch clamp amplifier was used in combination with the PULSE stimulation and data acquisition software (HEKA, Lambrecht, Germany). *X. laevis* oocyte currents were recorded by two-electrode voltage-clamp technique using a Turbo TEC 03 amplifier

(npi electronic GmbH, Tamm, Germany) and PULSE acquisition software. All electrophysiological experiments were performed at room temperature.

Solutions and Chemicals

HEK-293 and CHO Cells. The external Ringer solution contained 140 mM NaCl, 5 mM KCl, 0.8 mM $MgCl_2$, 1 mM $CaCl_2$, 10 mM HEPES, and 5 mM glucose; pH adjusted to 7.35 with NaOH. The standard pipette solution contained 140 mM KCl, 2 mM $MgCl_2$, 1 mM $CaCl_2$, 10 mM HEPES, and 2.5 mM EGTA [66 nM free Ca^{2+} as calculated with EQCAL software (Biosoft, Cambridge, UK)] pH adjusted to 7.35 with KOH.

***X. laevis* Oocytes.** Experiments were performed in external solution containing 91 mM NaCl, 5 mM KCl, 1 mM $MgCl_2$, 1 mM $CaCl_2$, 5 mM HEPES; pH adjusted to 7.4 with NaOH. Pipettes were filled with 3 M KCl solution.

N-[4-[[1-[2-(6-Methyl-2-pyridinyl)ethyl]-4-piperidinyl]carbonyl]phenyl]methanesulfonamide dihydrochloride (E-4031) was a generous gift from Eisai (Tokyo, Japan) and NS1643 was from NeuroSearch A/S (Ballerup, Denmark) or purchased from Tocris/Biozol (Eching, Germany). Stock solutions of E-4031 (10 mM in distilled water) and NS1643 (10 or 30 mM in dimethyl sulfoxide) were dissolved in external solution to yield the final concentrations.

Unless otherwise mentioned, HEK-293 cells were used as a heterologous mammalian expression system to examine the effects of the erg activator NS1643 on rerg1b channels. In one type of experiments, control measurements and measurements in the presence of NS1643 were performed on the same cells. In another type of experiments, control measurements and measurements in the prolonged presence (15–60 min) of NS1643 were performed on different cells. To analyze dose-dependent effects of NS1643 on the voltage dependence of activation and the amplitude of rerg1b currents, concentrations between 0.1 and 30 μM NS1643 were tested. Further experiments on rerg1b, rerg1a, and rerg1a/1b channels were performed with 10 μM NS1643. 30 μM NS1643 was used in experiments on herg1a and rerg1a channels expressed in *X. laevis* oocytes.

Data Analysis

Experimental data are given as means ± S.E.M., with n representing the number of experiments from different cells. Depending on the type of experiment, Student's two-tailed paired or unpaired t test was used to assess statistical significance indicated by $p < 0.05$, $p < 0.01$, and $p < 0.001$. Processing of the electrophysiological data were performed with PulseFit 8.65 (HEKA), Excel (Microsoft Corp., Redmond, WA) and SigmaPlot 11.0 (Systat Software, Inc., San Jose, CA).

To assess the voltage dependence of erg channel activation, normalized data were fitted with a Boltzmann equation: $y = 1/(1 + \exp(-(V - V_{0.5})/k))$, where $V_{0.5}$ is the potential of half-maximal erg current amplitude and k is the slope factor. The summarized data on the dose dependence of NS1643 effects given in Table 1 also include data from experiments presented in Mewe et al. (2008). The time course of activation was determined by an envelope-of-tail protocol. Tail current amplitudes were normalized to the maximal amplitude of the control experiments, and, apart from the first data points, data were fitted with a single exponential function yielding the time constant of activation (τ_{act}) and—for rerg1b analysis—a delay (d): $I(t) = I_{min} + (I_{max} - I_{min}) \times (1 - \exp((-t + d)/\tau_{act}))$, where t is the time and I is the current amplitude. The time constant of inactivation was obtained by fitting a single exponential function to decaying erg current traces: $I(t) = I_{min} + (I_{max} - I_{min}) \times \exp(-t/\tau_{inact})$, where t is the time and I is the current amplitude. For erg1b channels, time constants of recovery from inactivation ($\tau_{recovery}$) and deactivation (τ_{deact}) were obtained by fitting current traces with the sum of two exponential functions describing recovery from inactivation as well as subsequent deactivation. For erg1a and erg1a/1b channels, fit procedures with three exponential functions were used, yielding the time constant of recovery from inactivation ($\tau_{recovery}$) and the time constants for fast ($\tau_{deact,fast}$) and slow deactivation ($\tau_{deact,slow}$).

TABLE 1

Dose dependency of effects of NS1643 on the voltage dependence of activation and current amplitude of rerg1b channels heterologously expressed in HEK-293 cells

Data obtained from experiments as shown in Fig. 1 are given as means ± S.E.M.

NS1643 Concentration	$\Delta V_{0.5}$	Increase of Maximal Outward Current	Increase of Tail Current Amplitude
0.1 μM	−6.3 ± 3.0 mV (n = 5)	16 ± 10% (n = 5)	33 ± 23% (n = 5)
1 μM	−10.5 ± 2.3 mV (n = 6)**	52 ± 11% (n = 4)*	34 ± 11% (n = 6)*
10 μM	−33.4 ± 4.5 mV (n = 10)***	304 ± 77% (n = 7)**	283 ± 90% (n = 10)*
30 μM	−62.0 ± 10.0 mV (n = 4)*	121 ± 61% (n = 4)*	185 ± 20% (n = 4)*

$\Delta V_{0.5}$, shift in the potential for half-maximal current activation; n, number of experiments on different cells.
* $P < 0.05$.
** $P < 0.01$.
*** $P < 0.001$.

Results

Dose-Dependent Effects of NS1643 on rerg1b Channels. rerg1b currents were recorded in the same cells before (control) and after application of 0.1, 1, 10, or 30 μM NS1643. Representative rerg1b membrane currents elicited in a HEK-293 cell under control conditions, after application of 10 μM NS1643 and additional application of 10 μM E-4031, are displayed in Fig. 1A. Under control conditions, outward currents were evoked at depolarizing test pulse potentials more positive than approximately −40 mV. The amplitude of these rerg1b currents increased up to potentials of approximately +10 mV. Potentials that were more positive yielded lower amplitudes, resulting in a bell-shaped current-voltage curve (Fig. 1B), reflecting the inward rectification of erg channels resulting from slow activation and fast inactivation. As summarized in Table 1, the highest increase in erg1b current amplitude was observed after application of 10 μM NS1643, whereas higher NS1643 concentrations led to a less intense increase. Under control conditions, the steady-state amplitude was maximal at approximately +10 mV, and NS1643 induced a concentration-dependent shift in this maximum to more negative potentials (1 μM, +10 mV; 10 μM, −10 mV; 30 μM, −20 mV; Fig. 1B).

The typical hook-like shape of erg tail currents is evoked by rapid recovery from inactivation followed by relatively slower deactivation. Because the peak tail-current amplitude mirrors the amount of channels activated by the preceding test pulse, the voltage dependence of rerg1b channel activation was assessed by plotting the peak tail-current amplitudes against the prepulse potential. A Boltzmann function—comprising the isochronal activation curve of the rerg1b current—was fitted to the data points to determine the potential of half-maximal rerg1b channel activation ($V_{0.5}$) and the slope factor (k). As described previously (Mewe et al., 2008), the NS1643-induced erg1b current increase was accompanied by a strong shift in the voltage dependence of activation. The shift in half-maximal activation ($\Delta V_{0.5}$) was concentration-dependent and ranged from $\Delta V_{0.5} = -6.3 \pm 3.0$ mV (n = 5; $p = 0.105$) at 0.1 μM NS1643 to $\Delta V_{0.5} = -62.0 \pm 10.0$ mV (n = 4; $p = 0.023$) at 30 μM NS1643 (see Table 1). The control measurements yielded a $V_{0.5}$ value of −1.7 ± 1.3 mV (n = 25). The slope factor k did not change significantly at any of the tested NS1643 concentrations. In control experiments performed in the absence of drug, the voltage dependence of

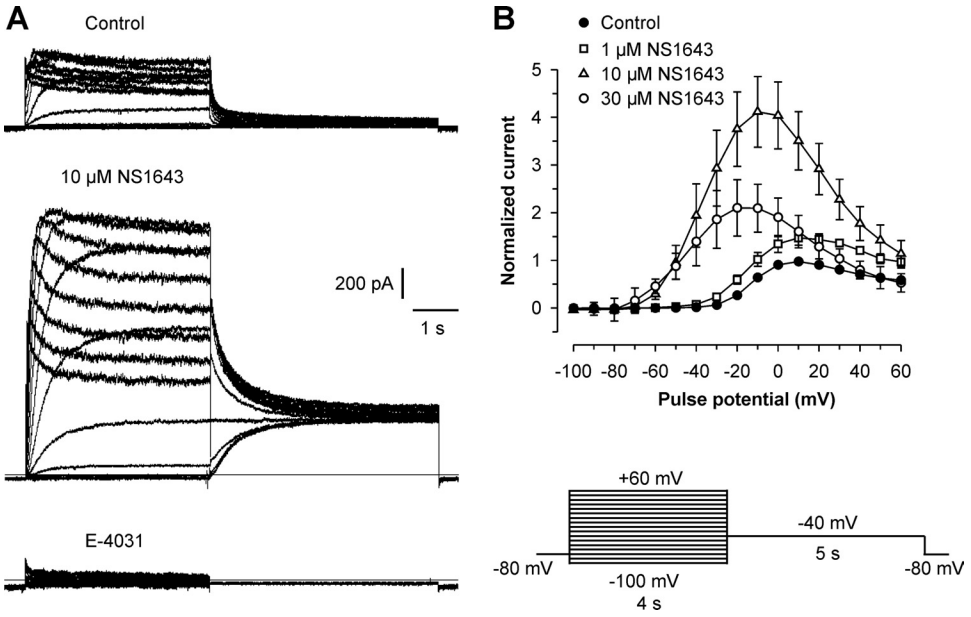

Fig. 1. NS1643 strongly activates rerg1b channels. Membrane currents were recorded in HEK-293 cells expressing rerg1b channels. Rat erg1b channel activation was assessed by 4-s depolarizing test pulses between −100 mV and +60 mV with 10-mV increments, followed by a constant pulse to −40 mV for 5 s (see pulse diagram). A, representative rerg1b current traces. Currents were measured in the same cell before (control) and after application of 10 μM NS1643 and 10 μM E-4031. B, current-voltage relationship of outward current amplitudes measured at the end of the depolarizing pulses under control conditions (n = 15) and after application of 1 μM (n = 4), 10 μM (n = 7) and 30 μM NS1643 (n = 4). For each experiment, current amplitudes were normalized to the maximum of the respective control. Data are means ± S.E.M.

erg1b activation did not significantly change with time during recordings with repeated pulse protocols (after establishment of the whole-cell configuration, $V_{0.5}$ = −2.7 ± 1.8 mV; after at least four complete pulse protocols and 13.8 ± 1.7 min later, $V_{0.5}$ = −5.6 ± 2.5 mV; n = 8; p = 0.14).

Because the leftward shift in the voltage dependence of activation steadily increased with higher concentrations of NS1643, the presence of an optimum of the NS1643 effect on erg1b current amplitude points to an additional channel blocking effect of NS1643 at higher concentrations as described previously for erg1a channels (Casis et al., 2006).

Time and Use Dependence of NS1643 Effects. To investigate and compare the time course of the two different agonistic effects of NS1643 on rerg1b channels, a special test pulse sequence was applied to obtain information for both, the shift in the voltage dependence of activation and the increase in amplitude (Fig. 2). During the first −40-mV test pulse, no significant rerg1b channel activation was obtained under control conditions. After application of 10 μM NS1643, increasing channel activation was detectable as a result of the slowly developing leftward shift in the voltage dependence of activation. The ratio of the maximal current amplitudes elicited with the first and the second potential step to −40 mV was used to determine the fraction of channels already activating at −40 mV. After application of NS1643, this fraction increased from approximately zero (no activation at −40 mV) to almost 1 (all channels already activated at −40 mV), serving as a nonlinear measure of the shift in the voltage dependence of activation. The tail-current amplitude normalized to its maximal value during the experiment was evaluated as second parameter. The time course of changes in erg1b current amplitude and of shifts in the voltage dependence of activation induced by application of 10 μM NS1643 was traced by repeating the test pulse sequence every 7 s. A representative family of current traces is displayed in Fig. 2A. Even though the time courses of the two different effects varied considerably between individual experiments, the shift in the voltage dependence of activation always required more time to reach a maximum than the increase in erg1b current amplitude (n = 5). In longer experiments, the current amplitude showed a tendency to decrease despite the continued presence of NS1643. In contrast, the shift in the voltage dependence of activation never reversed.

Use dependence of the NS1643 effects was tested in experiments including a 5-min interruption of the repeated test pulses at the time of application of 10 μM NS1643. After this 5-min interval at a holding potential of −80 mV, the test pulse sequence was applied again every 7 s (see Fig. 2B). With the first pulse sequence after the break, the increase in rerg1b tail-current amplitude was almost maximal, whereas the shift in the voltage dependence of activation had just partly developed and showed a strong increase with the next pulse sequences. A comparison of experiments with and without continuous pulsing suggests that the time course of the increase in amplitude might have been similar in both types of experiments, whereas the time course of the shift in the voltage dependence of activation differed considerably. With continuous pulsing, 50% of rerg1b channels could be activated at −40 mV after approximately 2.5 min (145.6 ± 21.6 s; n = 5); when NS1643 was applied at a constant negative potential of −80 mV, less than 50% (39 ± 8%; n = 6) of the rerg1b channels were activated at −40 mV during the first test pulse sequence 5 min after NS1643 application. This difference indicates a use dependence of the shift in the voltage dependence of activation by NS1643.

Effect of NS1643 on the Time Course of Activation of rerg1b Currents. The effect of NS1643 on rerg1b activation kinetics was investigated by an envelope of tail protocol. Depending on the duration of the depolarizing pulse, an increasing fraction of rerg1b channels activated, mirrored by the peak tail-current amplitude elicited by the hyperpolarizing pulse. Representative rerg1b current traces as well as averaged data before and after application of 10 μM NS1643 are shown in Fig. 3. The peak tail-current amplitudes before and after application of 10 μM NS1643 were normalized to the maximum control current and plotted against the duration of the preceding pulse. To identify the time constant of activation ($\tau_{activation}$), a single exponential function including a delay (d) was fitted to the data points. The delay was introduced to respect initial closed-closed transitions of the

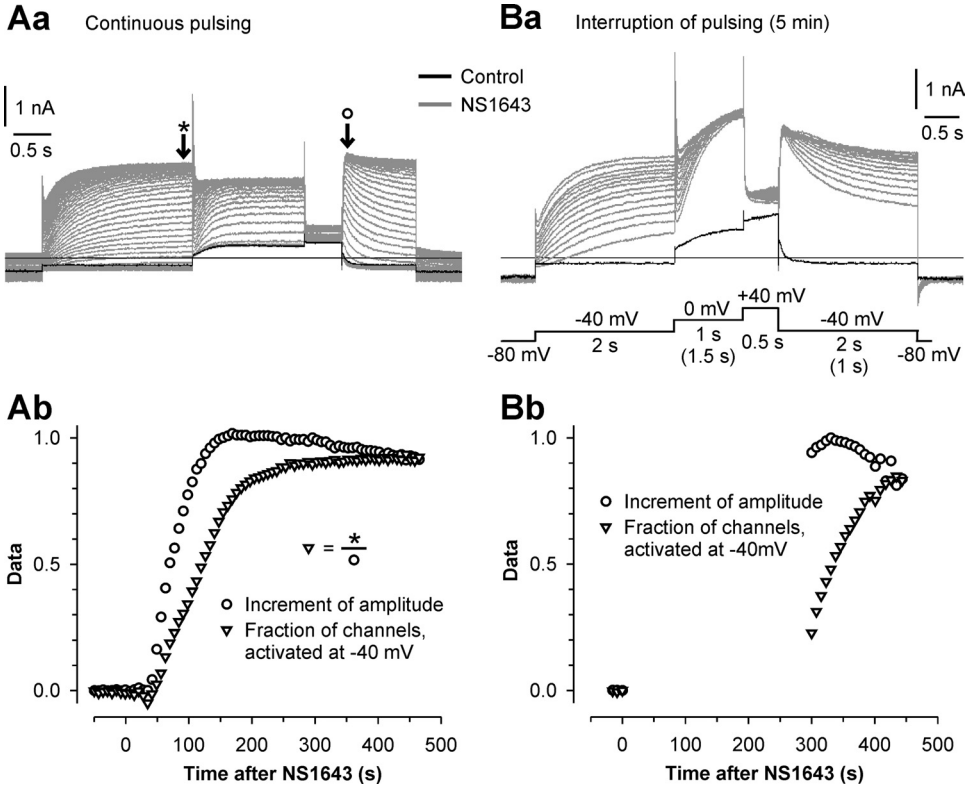

Fig. 2. Time course and use dependence of NS1643 effects. Rat erg1b currents were elicited in HEK-293 cells before and various time after the start of NS1643 application from a holding potential of −80 mV by the potential sequence shown in the pulse protocol. Each pulse sequence consisted of a 2-s pulse to −40 mV, followed by a step to 0 mV, a 0.5-s test pulse to 40 mV to achieve maximal channel activation, and a final second potential step to −40 mV to elicit maximal tail-current amplitudes. Some experiments were performed with slightly different pulse durations (see pulse protocol). After control runs of the test pulse sequence, application of 10 μM NS1643 was started and the pulse sequence was either repeated every 7 s or it started after a gap of 5 min at the holding potential of −80 mV. A and B, superimposed current traces and evaluation of an experiment with continuous pulsing (A) and of an experiment with interrupted pulsing (B). Control current traces are displayed in black. Gray traces have been recorded after the start of NS1643 application. Ab and Bb display the time courses of the increment in the tail-current amplitude as well as of the fraction of erg1b channels activated at the end of the first pulse to −40 mV, indicating a shift in the voltage dependence of activation. The tail-current amplitudes were measured at the second −40-mV test pulse (marked with a circle) and normalized to the maximum tail-current amplitude recorded in the presence of NS1643. The fraction of erg1b channels activated at −40 mV was defined as the quotient of the rerg current amplitude at the end of the first −40-mV test pulse (marked with an asterisk) and the peak tail-current amplitude at the second −40-mV test pulse of the same pulse sequence. This current ratio served as a nonlinear measure of the shift in the voltage dependence of erg1b channel activation.

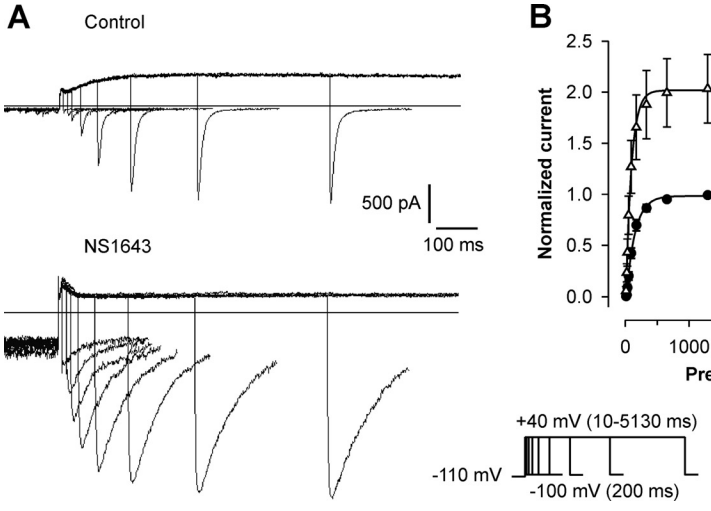

Fig. 3. Effect of NS1643 on the time course of activation of rerg1b channels. Membrane currents of HEK-293 cells expressing rerg1b channels were evoked by depolarizing pulses to +40 mV of increasing duration (between 10 and 5130 ms), followed by a 200-ms hyperpolarization to −100 mV. The holding potential was −110 mV (see pulse protocol). A, representative membrane currents of one cell before (Control) and after application of 10 μM NS1643. B, peak tail-current amplitudes were normalized to the maximum of the respective control, averaged and plotted against the duration of the preceding depolarizing pulse (n = 6). Mean data points were fitted with single exponential functions including a delay (Control, $\tau_{activation}$ = 136.9 ms, delay = 14.4 ms; NS1643, $\tau_{activation}$ = 88.5 ms, delay = 7.7 ms). Data are means ± S.E.M.

erg channels (see Wang et al., 1997; Gómez-Varela et al., 2002). Neither the time constant of activation nor the delay was significantly changed after the application of NS1643 ($\tau_{activation}$, 133.63 ± 23.82 ms for control, 109.34 ± 16.47 ms for NS1643, n = 6, p = 0.283; delay d, 21.44 ± 4.73 ms for control, −6.72 ± 13.47 ms for NS1643, n = 6, p = 0.139).

Effect of NS1643 on The Time Course of Recovery from Inactivation and Deactivation. The effect of 10 μM NS1643 on the time course of recovery from inactivation and deactivation was analyzed by an availability protocol (Fig. 4). Starting from the fully activated and predominantly inactivated state of the erg channels, the variable test pulses

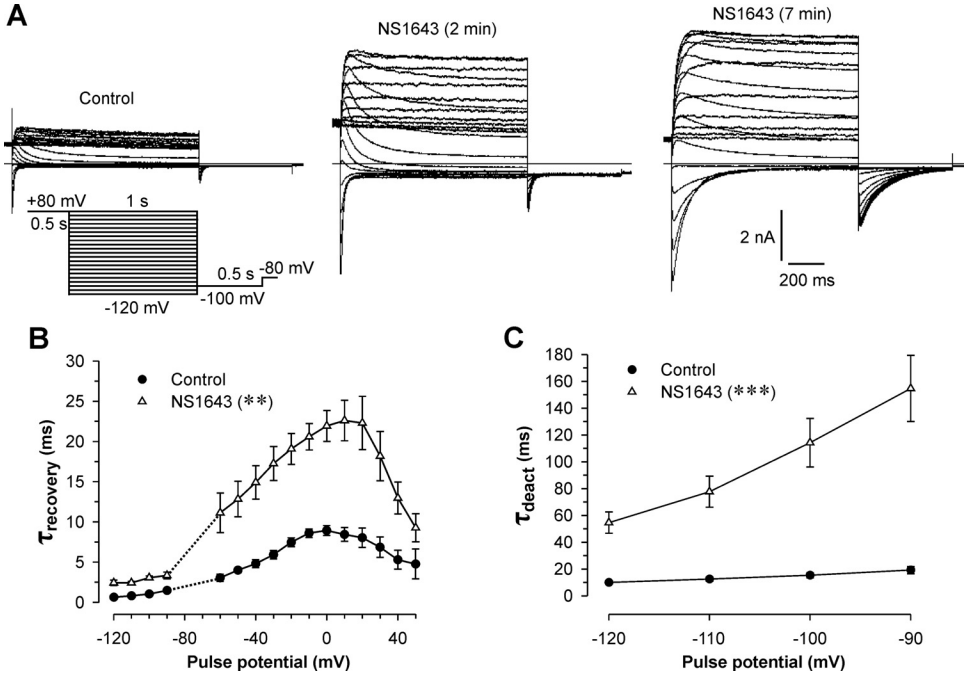

Fig. 4. Recovery from inactivation and deactivation kinetics of rerg1b channels are strongly slowed by NS1643. Membrane currents of HEK-293 cells heterologously expressing rerg1b channels were elicited by 0.5-s depolarizations to +80 mV followed by variable 1-s test pulses from +80 to −120 mV with 10-mV decrements (see pulse protocol). A, membrane currents from the same cell before (Control) as well as 2 and 7 min after the start of 10 μM NS1643 application. B, averaged time constants of recovery from inactivation ($\tau_{recovery}$) as a function of the pulse potential before and after application of 10 μM NS1643 ($n = 6$). NS1643 evoked a significant increase of $\tau_{recovery}$ (**, $p < 0.01$ for all displayed potentials, except for −60 mV, where $p < 0.05$). Data points for potentials close to the potassium equilibrium potential were omitted. C, time constants of deactivation (τ_{deact}) as a function of the test pulse potential ($n = 9$). NS1643 (10 μM) evoked a highly significant increase of τ_{deact} (***, $p < 0.001$ for all displayed potentials). Data points are means ± S.E.M.

induced voltage-dependent recovery from inactivation and deactivation. A single or double exponential function was fitted to the current traces, yielding the time constants of recovery from inactivation ($\tau_{recovery}$) and deactivation (τ_{deact}). Figure 4A shows rerg1b current traces obtained before and different time after the start of 10 μM NS1643 application. NS1643 induced a marked slowing of the time course of recovery from inactivation and deactivation, but the time course of these kinetic effects was delayed compared with the NS1643 effects on current amplitude and seemed to parallel the changes in the voltage dependence of activation. Under control conditions, $\tau_{recovery}$ ranged between 0.64 ± 0.08 ms at −120 mV and 8.97 ± 0.61 ms at 0 mV and increased by application of NS1643 to 2.43 ± 0.35 ms at −120 mV ($n = 6$; $p = 0.004$) and to 21.93 ± 1.93 ms at 0 mV ($n = 6$; $p = 0.001$; Fig. 4B). The slowing of deactivation kinetics, analyzed at pulse potentials between −120 and −90 mV, was even stronger: at −120 mV, τ_{deact} increased from 10.0 ± 1.1 (control) to 54.6 ± 7.9 ms (10 μM NS1643; $n = 9$; $p < 0.0001$), and at −90 mV, τ_{deact} changed from 19.2 ± 2.7 to 154.7 ± 24.7 ms ($n = 9$; $p < 0.0001$; Fig. 4C).

Effect of NS1643 on The Inactivation of rerg1b Channels. The time course of inactivation of rerg1b channels was investigated by a triple-pulse protocol. Starting from a holding potential of −80 mV, a 500-ms depolarizing pulse to +80 mV (P1) was used to fully activate and inactivate rerg1b channels. A 10-ms variable test pulse (P2) was then applied, leading to voltage-dependent recovery from inactivation, mirrored by the current amplitude elicited by a subsequent 150-ms depolarizing pulse to +60 mV (P3). erg current amplitudes elicited by P3 massively increased in the presence of NS1643, hampering proper voltage control. To reduce the influence of incomplete voltage control, we analyzed current traces with similar amplitude before and after NS1643 application. Monoexponential fits to the decay phase of P3 current traces yielded similar mean values of τ_{inact} of 4.7 ± 0.3 ms at +60 mV under control conditions and of 4.8 ± 0.4 ms ($n = 7$; $p = 0.976$) after application of 10 μM NS1643. The same type of pulse protocol was previously used to identify NS1643-induced shifts in the voltage dependence of inactivation of erg1a channels (Hansen et al., 2006). A similar evaluation was not appropriate for rerg1b because of the drastic increase in current amplitude and strong slowing of the recovery from inactivation (Fig. 4B), rendering a comparability of the data obtained before and after NS1643 application impossible.

Another attempt was made to assess the effect of NS1643 on rerg1b channel inactivation using the fully activated current-voltage relationship. Experiments were carried out either without or with prolonged presence of NS1643 in the bath to assess the "steady-state" effects of the drug on the inactivation of rerg1b channels. Problems associated with the pronounced NS1643-induced increase in erg1b current amplitudes were minimized by choosing the experiments for analysis to roughly match the current amplitudes in the two experimental groups (Fig. 5A, a and b). To account for a possible use dependence of the NS1643 effect, several pulse protocols preceded the one used for analysis in both groups. Figure 5B shows that the normalized fully activated current-voltage plots for the control and the NS1643 group were similar but not identical. Upon repolarizing potential steps between +80 and 0 mV, the voltage-dependent increase in erg1b current amplitude due to increased recovery from inactivation was almost identical. A deviation of the data occurred in the potential range where voltage-dependent deactivation affected the amplitudes of the control currents clearly more than the currents measured in the presence of NS1643, which is explained by the pronounced leftward shift in the activation curve. Mean peak current values of both groups served to calculate the relative erg1b conductance (Fig. 5C). Data in the potential range with no apparent or marginal deactivation were considered for fits with a Boltzmann function. It is noteworthy that the resulting $V_{0.5}$ values of −15.4 mV (control) and −13.4 mV (NS1643) are quite close to the reported potential for half-maximal steady-state inactivation of rerg1b channels obtained with a classic triple-

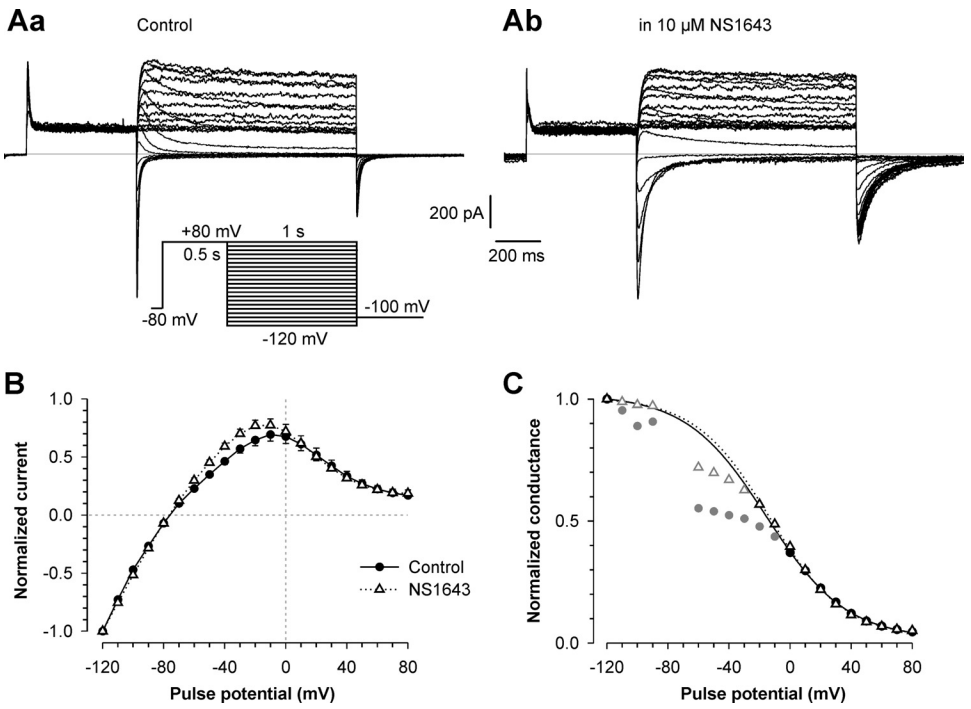

Fig. 5. Effect of NS1643 on the fully activated current-voltage relationship of rerg1b channels. Membrane currents of HEK-293 cells heterologously expressing rerg1b channels were recorded either under control conditions or with 10 μM NS1643 in the bath for at least 15 min. Experiments from different cells recorded without (Aa) or with (Ab) NS1643 were matched for similar rerg current amplitudes. The pulse protocol consisted of 0.5-s depolarizations to +80 mV to fully activate the channels, followed by variable 1-s test pulses from +80 to −120 mV with 10-mV decrement. B, peak current amplitudes (means ± S.E.M.; $n = 5$ for both control and NS1643) plotted against the test pulse potential. Before averaging, data were normalized to the maximum tail-current amplitude elicited with the test pulse to −120 mV. C, normalized conductance values were calculated from the mean current values given in B, using a reversal potential of −77.5 mV for control and for NS1643. Data points shown in gray were not considered for the Boltzmann fits (control, $V_{0.5} = -15.4$ mV, $k = -26.1$ mV; NS1643, $V_{0.5} = -13.4$ mV; $k = -24.5$ mV).

pulse protocol as described above (−16.2 mV; Kirchberger et al., 2006).

Effects of NS1643 on rerg1a and rerg1a/1b Channels. Because we found much stronger effects and a different mechanism of activation of rerg1b channels expressed in mammalian cells compared with the results on herg1a channels in *X. laevis* oocytes, we also investigated the effects of NS1643 on the voltage dependence of activation of rerg1a channels expressed in HEK-293 cells. Representative rerg1a current traces as well as averaged data before and after application of 10 μM NS1643 are shown in Fig. 6A. A clear shift in the voltage dependence of rerg1a activation was observed: $V_{0.5}$ changed from −18.9 ± 3.9 mV under control conditions to −45.7 ± 4.4 mV ($n = 6$; $p = 0.001$) after application of 10 μM NS1643. The slope factor k did not alter significantly. The increase in the peak tail-current amplitude by 39 ± 16% ($n = 6$; $p = 0.156$) was not significant, but the maximum outward current amplitude was clearly augmented by 136 ± 18% ($n = 6$; $p = 0.001$).

erg1a and erg1b subunits are coexpressed in many tissues and are able to form heteromeric channels (Jones et al., 2004; Guasti et al., 2005). Therefore, we also tested NS1643 on heteromeric erg1a/1b channels. Figure 6B illustrates the prominent activation of rerg1a/1b channels by 10 μM NS1643. $V_{0.5}$ shifted highly significant from −17.0 ± 2.7 mV under control conditions to −55.4 ± 2.1 mV ($n = 5$; $p < 0.0001$) after NS1643 application. The peak tail-current amplitudes and the maximum outward current amplitudes increased significantly by 89 ± 23% ($n = 5$; $p = 0.023$) and by 212 ± 34% ($n = 5$; $p = 0.003$), respectively.

Inspection of the rerg1a and rerg1a/1b tail currents suggested that NS1643 slowed the time course of deactivation of both types of erg1 channels (Fig. 6, Aa and Ba). Fits of the tail-current traces with the sum of three exponential equations allowed a more detailed analysis of the NS1643 effects, which are summarized in Table 2. NS1643 increased the time constant of recovery from inactivation for rerg1a and for rerg1a/1b. The slowing of rerg1a/1b channel deactivation included increases of the time constants for fast and slow deactivation as well as an increase in the relative contribution of the slowly deactivating current component. The observed slowing of rerg1a tail currents resulted from decelerated fast deactivation combined with an increase in the relative contribution of the slowly deactivating current component, although the time constant for the latter process decreased.

To ensure that the observed strong effects of NS1643 on rerg1b and rerg1a channels are not specific to HEK-293 cells, additional experiments concerning the voltage dependence of activation and the amplitude of steady-state outward and tail currents were performed in CHO cells, heterologously expressing rerg1b or rerg1a channels. In these experiments, 10 μM NS1643 also exerted strong activating effects, which did not differ from those observed in HEK cells (data not shown). The robust activating influence of NS1643 on rat erg1 channels is therefore reproducible in another mammalian expression system and is not specific to HEK-293 cells.

NS1643 Effects on herg1a Channels Expressed in CHO Cells. A single amino acid difference can be crucial for the effects of erg channel activators (Perry and Sanguinetti, 2008). To check whether the small sequence differences between herg1a and rerg1a channels might underlie the different sensitivity to NS1643 of rerg1 channels investigated in mammalian expression systems compared with herg1 channels expressed in *X. laevis* oocytes, we performed additional measurements on herg1a channels using stably transfected CHO cells. After confirming that short-term application of 10 μM NS1643 resulted in a considerable herg1a current increase, experiments were carried out either in the absence or with prolonged presence of NS1643 in the bath to assess the "steady-state" effects of the drug on the activation and inactivation of herg1a channels. As for rerg1b channels (data of Fig. 5), only part of the experiments were chosen for analysis to match the herg1a current amplitudes in the two experi-

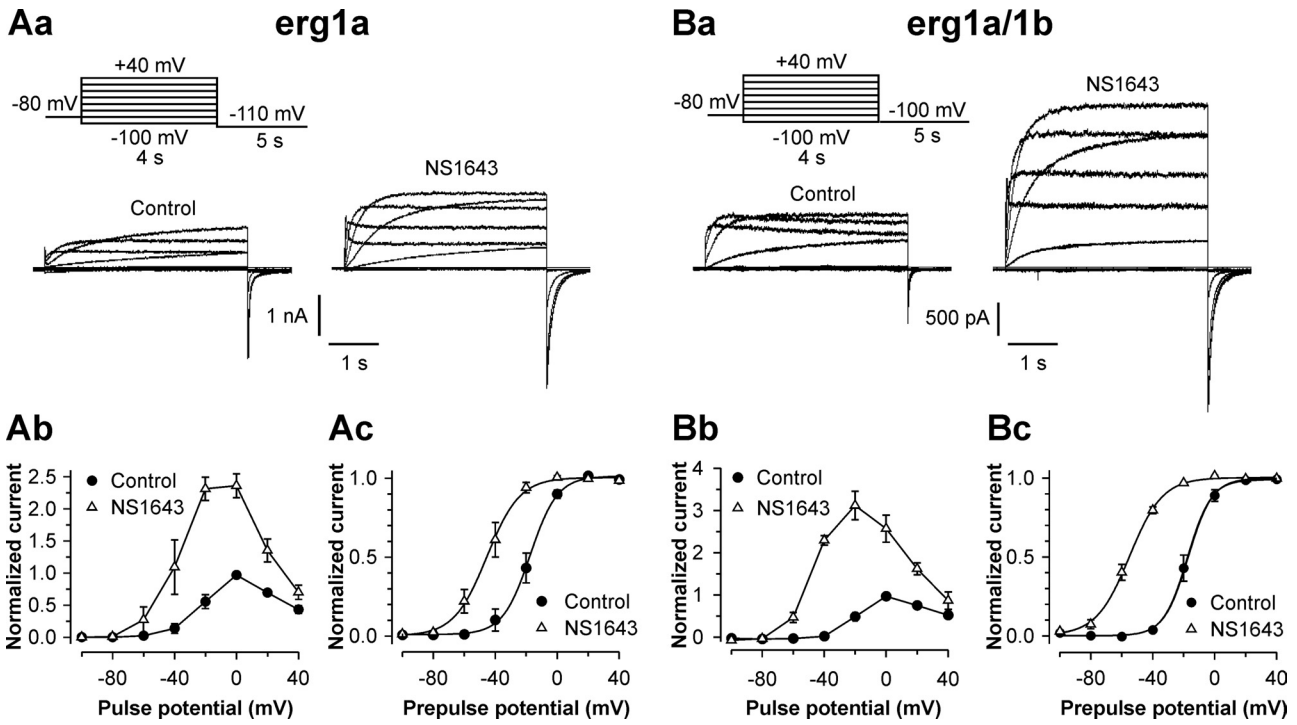

Fig. 6. Effects of NS1643 on current amplitude and voltage dependence of activation of rerg1a and rerg1a/1b channels expressed in HEK-293 cells. Membrane currents of HEK-293 cells heterologously expressing rerg1a (Aa) or rerg1a/1b (Ba) channels were elicited by variable 4-s depolarizing test pulses to potentials between −100 and +40 mV with 20-mV increments, followed by hyperpolarizations to −110 mV (rerg1a) or −100 mV (rerg1a/1b). The holding potential was −80 mV (see pulse protocols). Aa, representative rerg1a current traces recorded from the same cell before and after application of 10 μM NS1643. Ab, current-voltage relationship of rerg1a outward current amplitudes, measured at the end of the depolarizing test pulses. Current amplitudes before and after NS1643 application were normalized to the maximum control current and averaged (n = 6). Ac, peak tail-current amplitudes plotted against the potential of the preceding test pulse. Data points were normalized to the maximum tail-current amplitudes, averaged and fitted with a Boltzmann function, yielding the activation curves with the potentials of half-maximal activation, $V_{0.5}$ (control, $V_{0.5}$ = −17.5 mV; NS1643, $V_{0.5}$ = −45.4 mV; n = 6). Ba, rerg1a/1b current traces before and after application of 10 μM NS1643. Analyses of outward currents (Bb) and peak tail currents (Bc) (control, $V_{0.5}$ = −17.8 mV; NS1643, $V_{0.5}$ = −55.1 mV; n = 5) were performed as described in Ab and Ac. Data points are means ± S.E.M.

TABLE 2

Effects of 10 μM NS1643 on the time course of recovery from inactivation and of deactivation of rerg1a and rerg1a/1b channels heterologously expressed in HEK−293 cells

Data obtained from experiments as shown in Fig. 6 are given as means ± S.E.M. Tail currents were fitted with the sum of three exponential equations yielding the time constant of recovery from inactivation ($\tau_{recovery}$), the time constants of fast and slow deactivation ($\tau_{deact,fast}$ and $\tau_{deact,slow}$), and the relative contribution of the slowly deactivating current component ($S/(S + F)$).

	rerg1a at −110 mV (n = 5)		rerg1a/1b at −100 mV (n = 5)	
	Control	NS1643	Control	NS1643
$\tau_{recovery}$	1.90 ± 0.20 ms	2.94 ± 0.28 ms*	2.87 ± 0.21 ms	4.42 ± 0.42 ms
$\tau_{deact,fast}$	27.1 ± 4.9 ms	82.8 ± 11.6 ms**	26.9 ± 2.9 ms	139.0 ± 36.28 ms*
$\tau_{deact,slow}$	278.0 ± 26.7 ms	219.4 ± 20.6 ms*	164.9 ± 39.2 ms	461.6 ± 76.3 ms*
$S/(S + F)$	11 ± 1%	34 ± 4%*	18 ± 4%	34 ± 13%

n, number of experiments on different cells.
* $P < 0.05$.
** $P < 0.01$.
*** $P < 0.001$.

mental groups (Figs. 7 and 8). With prolonged exposure to 10 μM NS1643, the voltage dependence of herg1a channel activation was shifted by almost 30 mV to more negative potentials (Fig. 7, A and B). The differences in the potential for half-maximal activation between the two groups were highly significant (control, $V_{0.5}$ = −28.3 ± 1.3, n = 9; NS1643, $V_{0.5}$ = −55.3 ± 2.1, n = 8; $p < 0.0001$).

In contrast to the results on erg1b channels, these changes in the voltage dependence of activation were associated with a pronounced acceleration of herg1a current activation (Fig. 7, C and D). Time constants of activation were determined for three different potentials with an envelope of tail protocol as described for erg1b. In the presence of 10 μM NS1643, the values of $\tau_{activation}$ amounted only to approximately half of the control values (Fig. 7D).

As a measure of steady-state inactivation, the relative herg1a conductance was calculated from the fully activated current-voltage relationship (Fig. 8). The normalized peak amplitudes of the herg1a currents were almost identical for the control group and the cells recorded with NS1643 in the bath (Fig. 8B). Accordingly, the conductance curves were strikingly similar (Fig. 8C), suggesting that the voltage dependence of herg1a inactivation was not altered by prolonged exposure to 10 μM NS1643.

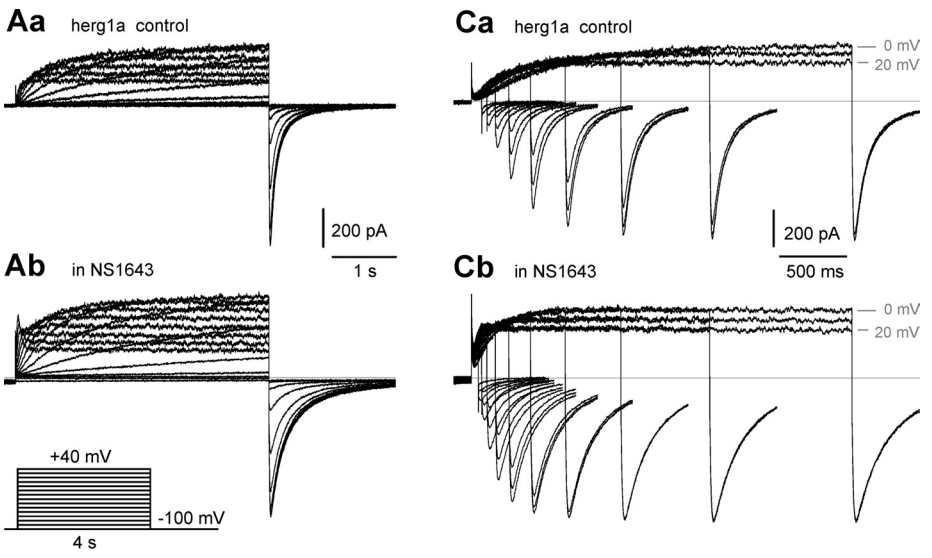

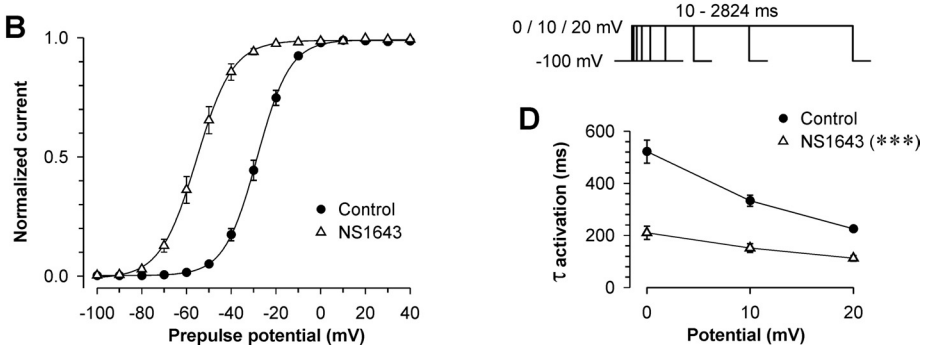

Fig. 7. Effect of NS1643 on the voltage dependence and time course of activation of herg1a channels. Human erg1a currents were recorded from stably transfected CHO cells under control conditions or with 10 μM NS1643 in the bath for at least 15 min. Experiments from different cells recorded with or without NS1643 were matched for similar herg current amplitudes. Aa and Ab, erg currents were elicited by variable 4-s depolarizing test pulses to potentials between −100 and +40 mV with 10-mV increments, followed by repolarization to the holding potential of −100 mV. B, peak tail-current amplitudes plotted against the potential of the preceding test pulse. Data points were normalized to the maximum tail-current amplitudes, averaged, and fitted with a Boltzmann function, yielding the activation curves with the potentials of half-maximal activation, $V_{0.5}$ (control, $V_{0.5} = -28.4$ mV, $n = 9$; NS1643, $V_{0.5} = -55.5$ mV, $n = 8$). C, herg1a currents evoked by an envelope-of-tail protocol without (Ca) or with (Cb) NS1643 in the bath. From a holding potential of −100 mV, depolarizing pulses to 0, 10, or 20 mV of increasing duration (between 10 and 2824 ms) were applied followed by repolarization to −100 mV (see pulse protocol). D, time constants (means ± S.E.M.) of herg1a channel activation as function of the membrane potential. Data are derived from experiments without ($n = 9$) or with NS1643 ($n = 7$) as shown in C. In the presence of 10 μM NS1643, $\tau_{activation}$ was significantly decreased (***, $p < 0.001$ for all three potentials).

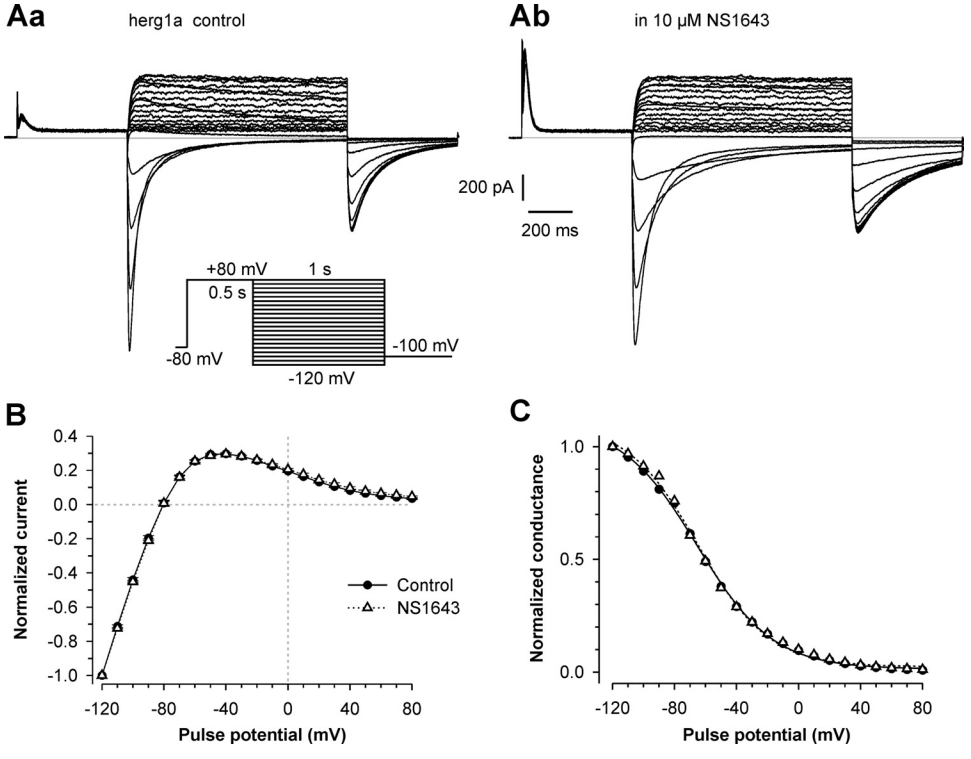

Fig. 8. Effect of NS1643 on the fully activated current-voltage relationship of herg1a channels. Human erg1a currents were recorded from stably transfected CHO cells either under control conditions or with 10 μM NS1643 in the bath for at least 15 min. Experiments from different cells recorded without (Aa) or with (Ab) NS1643 were matched for similar herg current amplitudes. The pulse protocol consisted of 0.5-s depolarizations to +80 mV to fully activate the erg channels, followed by variable 1-s test pulses from +80 to −120 mV with 10 mV decrements. B, peak current amplitudes are plotted against the test pulse potential to yield the fully activated current-voltage relationship. Data are means ± S.E.M. ($n = 7$ for control and $n = 6$ for NS1643). Before averaging, data were normalized to the maximum tail-current amplitude elicited with the test pulse to −120 mV. C, normalized conductance values derived from the mean current values given in B were fitted with a Boltzmann function (control, $V_{0.5} = -65.4$ mV, $k = -24.5$ mV; NS1643, $V_{0.5} = -64.9$ mV; $k = -22.9$ mV). Conductance was calculated using a reversal potential of −80.4 mV for both control and NS1643.

Impact of the Expression System and Presence of Beta Subunits on the NS1643 Effect. herg1a and rerg1a channels were heterologously expressed in *X. laevis* oocytes, and some comparative measurements were performed using 30 μM NS1643. Representative current traces and data analyses, displayed in Fig. 9, illustrate a moderate activating

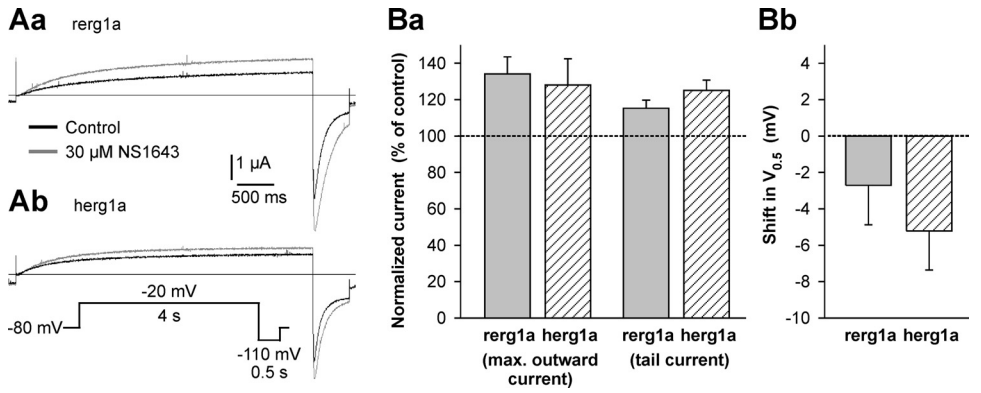

Fig. 9. Effect of NS1643 on rerg1a and herg1a channels expressed in *X. laevis* oocytes. A, representative current traces measured in *X. laevis* oocytes heterologously expressing rerg1a (Aa) and herg1a (Ab) channels elicited by the indicated pulse protocol before (black) and after (gray) application of 30 μM NS1643. Ba, mean rerg1a ($n = 3$) and herg1a ($n = 3$) current amplitudes after application of 30 μM NS1643 normalized to the respective control. Maximum outward currents were determined by an activation protocol consisting of variable 4-s test pulses between −90 and +60 mV, followed by a hyperpolarization to −110 mV. Peak tail-current amplitudes were determined by hyperpolarizations to −110 mV after test pulses to −20 mV. Bb, mean shift in the potential of half-maximal activation ($V_{0.5}$) of rerg1a and herg1a channels by 30 μM NS1643. $V_{0.5}$ values were determined by fitting Boltzmann functions to the tail-current amplitudes obtained with the activation protocol explained in Ba. Data are means ± S.E.M.

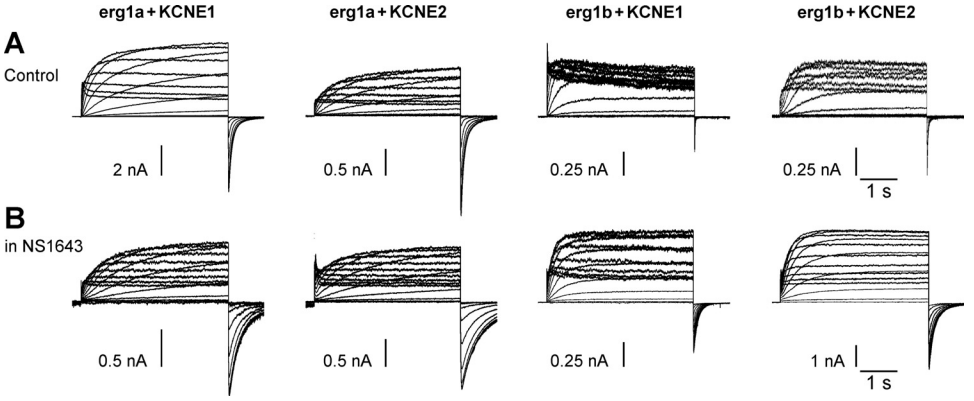

Fig. 10. Coexpression of KCNE beta subunits with erg1a and erg1b. Membrane currents of HEK-293 cells expressing different combinations of rat erg1a or erg1b and rat KCNE1 or KCNE2. erg currents were elicited from a holding potential of −80 mV by variable 4-s depolarizing test pulses up to +40 mV with 10 mV increments, followed by a hyperpolarization to −100 mV. Families of membrane currents evoked in the absence (A) or presence (B) of 10 μM NS1643 were recorded from different cells. Data analysis is given in Table 3.

effect of NS1643 on erg1 channels expressed in *X. laevis* oocytes as described previously (Casis et al., 2006; Hansen et al., 2006). The increase of maximum outward current was 34.1 ± 9.4% for rerg1a ($n = 3$; $p = 0.068$) and 28.0 ± 14.4% for herg1a ($n = 3$; $p = 0.191$). Even with long application periods, a significant shift in the voltage dependence of activation was observed for neither rerg1a nor herg1a channels [rerg, $V_{0.5;\ \mathrm{control}} = -30.5 \pm 1.2$ mV; $V_{0.5;\ \mathrm{NS1643}} = -33.2 \pm 2.6$ mV ($n = 3$; $p = 0.337$); herg, $V_{0.5;\ \mathrm{control}} = -28.5 \pm 2.7$ mV; $V_{0.5;\ \mathrm{NS1643}} = -33.7 \pm 1.0$ mV ($n = 3$; $p = 0.136$)]. The inward tail-current amplitudes of rerg1a and herg1a channels determined after a test pulse potential of −20 mV were augmented by 15.3 ± 4.5% (rerg1a; $n = 3$; $p = 0.057$) and 25.1 ± 5.6% (herg1a; $n = 3$; $p = 0.019$) after application of 30 μM NS1643 (see Fig. 9). These data confirmed that the effects of NS1643 on erg1a channels do not differ between human and rat isoforms and that the effects of NS1643 are much less intense on erg1 channels measured in oocytes compared with erg1 channels in a mammalian expression system.

X. laevis oocytes endogenously express members of the membrane-spanning KCNE family, which might influence the pharmacological properties of erg channels (Cui et al., 2001; Witchel et al., 2002; Anantharam et al., 2003). We coexpressed KCNE1 and KCNE2 together with rerg1a and rerg1b in HEK-293 cells to investigate whether these β-subunits would be able to attenuate the strong leftward shift in the voltage dependence of activation induced by NS1643. Rat erg1a and erg1b current measurements were performed without and with coexpression of KCNE1 and KCNE2 and in the absence or prolonged presence of 1 or 10 μM NS1643 (Fig. 10). The results of these experiments are summarized in Table 3. Even in the prolonged presence of NS1643, the effects on the voltage dependence of activation were more pronounced for erg1b than for erg1a. With 1 μM NS1643, $V_{0.5}$ values differed from control values by approximately 10 mV for erg1a and by approximately 25 mV for erg1b. With 10 μM NS1643, these differences amounted to approximately 30 mV for erg1a and approximately 40 mV for erg1b.

Cotransfection with the β-subunits had no apparent effect on the macroscopic currents and did not significantly change the voltage dependence of activation of erg1a or erg1b channels. In addition, the effectiveness of NS1643 on erg1a or erg1b channels was similar upon coexpression of the KCNE β-subunits. With 1 μM NS1643 in the bath, all $V_{0.5}$ values were significantly shifted to more negative potentials compared with the $V_{0.5}$ control values. Using a concentration of 10 μM NS1643, the voltage dependence of activation was shifted yet further to negative potentials. In contrast to the lack of an apparent effect on erg currents, KCNE1 cotransfection with KCNQ1 resulted in pronounced increases in current amplitude and slowing of KCNQ1 current activation demonstrating effective expression of the beta subunit (data not shown).

TABLE 3

Effects of 1 and 10 μM NS1643 on the voltage dependence of activation of rat erg1a and erg1b channels with and without coexpression of KCNE1 and KCNE2 in HEK-293 cells

Data obtained from analysis of experiments as shown in Fig. 10 are given as means ± S.E.M. Significance of differences in $V_{0.5}$ is given for 1 μM versus control and for 10 μM versus 1 μM NS1643.

	Control		1 μM NS1643		10 μM NS1643	
	$V_{0.5}$	k	$V_{0.5}$	k	$V_{0.5}$	k
	mV		*mV*		*mV*	
erg1a	−24.1 ± 1.8	8.5 ± 0.5 (n = 9)	−32.9 ± 2.2**	8.2 ± 0.6 (n = 7)	−53.6 ± 3.3***	8.7 ± 0.5 (n = 5)
+ KCNE1	−20.6 ± 2.5	8.3 ± 0.4 (n = 13)	−31.5 ± 2.5**	7.5 ± 0.4 (n = 8)	−51.3 ± 2.9***	8.4 ± 0.2 (n = 5)
+ KCNE2	−20.1 ± 1.8	7.9 ± 0.2 (n = 10)	−33.8 ± 2.1***	7.2 ± 0.4 (n = 11)	−54.6 ± 0.9***	7.3 ± 0.6 (n = 4)
erg1b	−1.5 ± 1.5	11.7 ± 0.5 (n = 10)	−27.6 ± 3.8***	8.6 ± 1.4 (n = 5)	−42.7 ± 3.2*	10.7 ± 1.8 (n = 4)
+ KCNE1	−2.3 ± 2.0	9.7 ± 0.6 (n = 6)	−29.1 ± 2.3***	8.7 ± 1.3 (n = 5)	−37.2 ± 2.0*	13.7 ± 0.9 (n = 4)
+ KCNE2	−4.6 ± 3.6	13.3 ± 2.2 (n = 6)	−17.9 ± 1.2*	9.6 ± 0.5 (n = 4)	−44.3 ± 4.6***	14.2 ± 0.7 (n = 6)

$V_{0.5}$, potential for half-maximal current activation; k, slope factor; n, number of experiments.
* $P < 0.05$.
** $P < 0.01$.
*** $P < 0.001$.

Discussion

We recently described that NS1643 exerts remarkable activating effects on rat erg1b channels expressed in HEK-293 cells (Mewe et al., 2008). We have now investigated the NS1643-induced changes in the biophysical properties of erg1b channels in more detail, and we performed comparative experiments on rat and human erg1a channels demonstrating that the small species differences (Bauer et al., 1998) cannot account for reported differences between herg1a data obtained in oocytes and rerg1b data obtained in HEK-293 cells. Using mainly HEK-293 cells as mammalian expression system, we found that rat erg1b current amplitudes increased in a dose-dependent manner up to 4-fold at a concentration of 10 μM NS1643. The most obvious changes in the biophysical properties suited to contribute to the massive current increase were the pronounced leftward shift in the voltage dependence of activation and the marked slowing of deactivation. Although a little less pronounced, both effects of NS1643 could also be elicited on erg1a channels when expressed in HEK or CHO cells. We were surprised to find that erg1b and erg1a channel inactivation in these mammalian cell lines was not altered by incubation with 10 μM NS1643.

NS1643 Effects in Different Expression Systems. The present data confirm and extend our previous results (Mewe et al., 2008) that NS1643 induces a dose-dependent dramatic shift in the voltage dependence of activation of rerg1b channels to more negative potentials. We now show that this pronounced leftward shift is also an important mechanism of channel activation by NS1643 of homomeric erg1a and heteromeric erg1a/1b channels when expressed in mammalian cells. The additional experiments performed in *X. laevis* oocytes confirmed that NS1643 affects erg1 channels much less intense in the oocyte system than in mammalian cells. These results obtained with 30 μM NS1643 are in good accordance with previously published data, which show variable effects on the voltage dependence of herg1a activation in oocytes, ranging from no significant shift (Casis et al., 2006; Hansen et al., 2006) up to a leftward shift by approximately 9 mV (Larsen et al., 2010). In addition, in oocytes, a negative shift in $V_{0.5}$ of herg1a activation seems to be concentration-dependent, and it is therefore more apparent with the higher NS1643 concentration of 60 μM (Xu et al., 2008).

For a huge number of erg blocking substances, erg channels expressed in oocytes are known to exhibit a lower drug sensitivity than erg channels expressed in mammalian cells. This lower sensitivity is readily explained by the size of the oocytes and the presence of yolk particles (Witchel et al., 2002; Polak et al., 2009). Nevertheless, other mechanisms might contribute to the observed differences in the potency of NS1643 to shift erg1 channel activation. *X. laevis* oocytes endogenously express members of the KCNE family that have been shown to influence some of the biophysical and pharmacological properties of erg channels (Cui et al., 2001; Anantharam et al., 2003; Bett and Rasmusson, 2008). We therefore tested whether coexpressed KCNE subunits attenuate the NS1643-induced leftward shift of erg1 channel activation in HEK-293 cells. In these experiments, coexpression of the β-subunits KCNE1 and KCNE2 had no effect on the sensitivity of erg1a and erg1b channels to NS1643, suggesting that endogenous KCNE subunits do not significantly contribute to the lower potency of NS1643 in *X. laevis* oocytes.

Significant effects of NS1643 on erg1b gating kinetics concerned the recovery from inactivation and the deactivation process. Because the slowing of deactivation was clearly more pronounced than the slowing of the recovery process, these changes should contribute to the NS1643-induced increase in erg tail-current amplitude. A significant increase in the time constants for recovery from inactivation and for deactivation was also found for erg1a and erg1a/1b channels, expressed in HEK-293 cells. In *X. laevis* oocytes, varying effects of NS1643 on erg1a channel deactivation have been observed, including no significant effect (Hansen et al., 2006), moderate slowing (Casis et al., 2006; Larsen et al., 2010), and more pronounced slowing of deactivation (Xu et al., 2008).

The fully activated current-voltage relationship was used to estimate the effect of NS1643 on erg1b steady-state inactivation. Despite the fact that the calculated conductance values followed a sigmoidal voltage dependence only at potentials with no or marginal current deactivation, neither the results of the Boltzmann fits nor the fully activated current-voltage plots pointed to a rightward shift in the erg1b steady-state inactivation curve by NS1643. This interpretation is supported by the surprising finding that the corresponding conductance-voltage relationship determined for herg1a channels was clearly unaffected by 10 μM NS1643. Thus, our present results on erg1a and erg1b channels clearly differ

from the findings on erg1a channels expressed in oocytes, where a shift in the voltage dependence of inactivation to more positive potentials (Casis et al., 2006; Hansen et al., 2006) and a reduced rate of inactivation (Xu et al., 2008) were described as main mechanisms of activation.

Higher Sensitivity to NS1643 of erg1b Compared with erg1a Channels. The activating effects of NS1643 were considerably stronger on erg1a channels expressed in HEK or CHO cells than those exerted in the oocyte system. Nevertheless, most NS1643-induced changes in the biophysical properties of erg1a channels were not as pronounced as for erg1b channels. This applies to the magnitude of the leftward shift in the activation curves, to the increase in steady-state and tail-current amplitudes, as well as to the slowing of channel deactivation. The only exception was the time course of activation, where erg1a exhibited a marked increase in the rate of activation when measured in the presence of 10 μM NS1643. In contrast, application of NS1643 did not significantly change the rate of erg1b channel activation. In oocyte experiments on herg1a, accelerated activation has been described mostly in combination with the presence of a NS1643-induced leftward shift of the activation curve (Xu et al., 2008; Larsen et al., 2010).

We also investigated the effects of NS1643 on erg1a/1b channels, because erg1a and erg1b subunits are often coexpressed and tend to form heteromeric channels (Lees-Miller et al., 1997; London et al., 1997; Jones et al., 2004; Kirchberger et al., 2006). Rat erg1a/1b channels exhibited a robust NS1643-induced increase in current amplitude, which was in between the results obtained for the corresponding homomeric channels. With almost −40 mV, the shift in the activation curve was similarly strong as for erg1b. Taken together, the present results show that the erg1b isoform is more sensitive to NS1643 than erg1a channels. This is in accordance with the recent finding that also herg1b channels expressed in oocytes are more sensitive than herg1a to NS1643 (Larsen et al., 2010).

Mechanism of Action of NS1643. The present experiments with NS1643 and erg1b channels revealed differences in the time course and in the use dependence of the increase in current amplitude and the shift in the voltage dependence of activation, indicating the existence of more than one mechanism of channel activation. Use dependence of herg current inhibition is a common feature of several erg blockers, which preferentially block open channels, and many of them require channel inactivation for high-affinity binding (for review, see Li and Dong, 2010). Nevertheless, in our experiments with NS1643, almost maximal increase in current amplitude was evident with the first pulse sequence after a prolonged period at a negative holding potential, suggesting efficient binding of NS1643 to erg1b channels in the closed state, as has been recently shown for 3-nitro-*N*-(4-phenoxyphenyl) benzamide (ICA-105574) (Gerlach et al., 2010).

Similar to findings in herg1a channels in oocytes (Casis et al., 2006), a very high concentration of NS1643 led to a less intense increment in erg1b currents with a more pronounced attenuation of the agonist activity at more positive potentials. This effect, which occurred at 100 μM in oocytes and at 30 μM in the present study, was interpreted as an additional erg channel blocking property of NS1643 (Casis et al., 2006). Phe656 of herg1a, a residue that interacts with most classic herg blockers, was suggested as a possible low-affinity binding site. Thus, different binding sites for NS1643 seem to exist in erg1a channels, suggesting that NS1643 possibly acts from both the external (Xu et al., 2008; Grunnet et al., 2011) and internal sides of the membrane. The presence of different binding sites would also well explain the differences in the time course and use dependence of the increase in current amplitude and the shift in the voltage dependence of activation found for erg1b channels in the present study.

Our experiments did not identify which additional mechanism—apart from the leftward shift in activation and slowing of deactivation—is involved in the observed increase in erg1b current amplitude, because erg1b channel inactivation was not affected by NS1643. Other possible mechanisms that could contribute to the drug-induced increase in erg whole-cell current are an enhanced maximal channel open probability or a reduced erg channel affinity to external Na^+, thus reducing the Na^+ block suggested to underlie the paradoxical agonist effect of external K^+ on herg current amplitude (Numaguchi et al., 2000; Mullins et al., 2002).

The slow time course of the NS1643-induced leftward shift in the activation curves of erg1a and erg1b channels combined with its use dependence could underlie the fact that it has not been observed or described in other studies also using mammalian cells as expression system or in experiments on native erg1 channels of cardiac myocytes. Future experiments with prolonged exposure to NS1643 could clarify this issue and would perhaps help to understand the in vivo effects of the drug.

Acknowledgments

We thank Annett Hasse, Margrit Hölzel, and Telse Kock for continuous support in the laboratory.

Authorship Contributions

Participated in research design: Schuster and Bauer.
Conducted experiments: Schuster, Glassmeier, and Bauer.
Performed data analysis: Schuster, Glassmeier, and Bauer.
Wrote or contributed to the writing of the manuscript: Schuster and Bauer.

References

Anantharam A, Lewis A, Panaghie G, Gordon E, McCrossan ZA, Lerner DJ, and Abbott GW (2003) RNA interference reveals that endogenous *Xenopus* MinK-related peptides govern mammalian K^+ channel function in oocyte expression studies. *J Biol Chem* **278:**11739–11745.

Bauer CK, Engeland B, Wulfsen I, Ludwig J, Pongs O, and Schwarz JR (1998) RERG is a molecular correlate of the inward-rectifying K current in clonal rat pituitary cells. *Receptors Channels* **6:**19–29.

Bett GC and Rasmusson RL (2008) Modification of K^+channel-drug interactions by ancillary subunits. *J Physiol* **586:**929–950.

Casis O, Olesen SP, and Sanguinetti MC (2006) Mechanism of action of a novel human *ether-a-go-go*-related gene channel activator. *Mol Pharmacol* **69:**658–665.

Cui J, Kagan A, Qin D, Mathew J, Melman YF, and McDonald TV (2001) Analysis of the cyclic nucleotide binding domain of the HERG potassium channel and interactions with KCNE2. *J Biol Chem* **276:**17244–17251.

Diness TG, Yeh YH, Qi XY, Chartier D, Tsuji Y, Hansen RS, Olesen SP, Grunnet M, and Nattel S (2008) Antiarrhythmic properties of a rapid delayed-rectifier current activator in rabbit models of acquired long QT syndrome. *Cardiovasc Res* **79:**61–69.

Fermini B and Fossa AA (2003) The impact of drug-induced QT interval prolongation on drug discovery and development. *Nat Rev Drug Discov* **2:**439–447.

Gerlach AC, Stoehr SJ, and Castle NA (2010) Pharmacological removal of human ether-a-go-go-related gene potassium channel inactivation by 3-nitro-N-(4-phenoxyphenyl) benzamide (ICA-105574). *Mol Pharmacol* **77:**58–68.

Gómez-Varela D, de la Peña P, García J, Giráldez T, and Barros F (2002) Influence of amino-terminal structures on kinetic transitions between several closed and open states in human erg K^+channels. *J Membr Biol* **187:**117–133.

Grunnet M, Abbruzzese J, Sachse FB, and Sanguinetti MC (2011) Molecular determinants of human ether–go-go-related gene 1 (hERG1) K^+channel activation by NS1643. *Mol Pharmacol* **79:**1–9.

Grunnet M, Hansen RS, and Olesen SP (2008) hERG1 channel activators: a new anti-arrhythmic principle. *Prog Biophys Mol Biol* **98:**347–362.

Guasti L, Cilia E, Crociani O, Hofmann G, Polvani S, Becchetti A, Wanke E, Tempia F, and Arcangeli A (2005) Expression pattern of the ether-a-go-go-related (ERG) family proteins in the adult mouse central nervous system: evidence for coassembly of different subunits. *J Comp Neurol* **491:**157–174.

Hansen RS, Diness TG, Christ T, Demnitz J, Ravens U, Olesen SP, and Grunnet M (2006) Activation of human ether-a-go-go-related gene potassium channels by the diphenylurea 1,3-bis-(2-hydroxy-5-trifluoromethyl-phenyl)-urea (NS1643). *Mol Pharmacol* **69:**266–277.

Hirdes W, Schweizer M, Schuricht KS, Guddat SS, Wulfsen I, Bauer CK, and Schwarz JR (2005) Fast erg K^+currents in rat embryonic serotonergic neurones. *J Physiol* **564:**33–49.

Jones EM, Roti Roti EC, Wang J, Delfosse SA, and Robertson GA (2004) Cardiac I_{Kr} channels minimally comprise hERG 1a and 1b subunits. *J Biol Chem* **279:**44690–44694.

Killeen MJ, Thomas G, Olesen SP, Demnitz J, Stokoe KS, Grace AA, and Huang CL (2008) Effects of potassium channel openers in the isolated perfused hypokalaemic murine heart. *Acta Physiol* (*Oxf*) **193:**25–36.

Kirchberger NM, Wulfsen I, Schwarz JR, and Bauer CK (2006) Effects of TRH on heteromeric rat erg1a/1b K^+channels are dominated by the rerg1b subunit. *J Physiol* **571:**27–42.

Larsen AP, Bentzen BH, and Grunnet M (2010) Differential effects of Kv11.1 activators on Kv11.1a, Kv11.1b and Kv11.1a/Kv11.1b channels. *Br J Pharmacol* **161:**614–628.

Lees-Miller JP, Kondo C, Wang L, and Duff HJ (1997) Electrophysiological characterization of an alternatively processed ERG K^+channel in mouse and human hearts. *Circ Res* **81:**719–726.

Li GR and Dong MQ (2010) Pharmacology of cardiac potassium channels. *Adv Pharmacol* **59:**93–134.

London B, Trudeau MC, Newton KP, Beyer AK, Copeland NG, Gilbert DJ, Jenkins NA, Satler CA, and Robertson GA (1997) Two isoforms of the mouse ether-a-go-go-related gene coassemble to form channels with properties similar to the rapidly activating component of the cardiac delayed rectifier K^+current. *Circ Res* **81:**870–878.

Lu HR, Vlaminckx E, Hermans AN, Rohrbacher J, Van Ammel K, Towart R, Pugsley M, and Gallacher DJ (2008) Predicting drug-induced changes in QT interval and arrhythmias: QT-shortening drugs point to gaps in the ICHS7B Guidelines. *Br J Pharmacol* **154:**1427–1438.

Mewe M, Wulfsen I, Schuster AM, Middendorff R, Glassmeier G, Schwarz JR, and Bauer CK (2008) Erg K^+channels modulate contractile activity in the bovine epididymal duct. *Am J Physiol Regul Integr Comp Physiol* **294:**R895–R904.

Mullins FM, Stepanovic SZ, Desai RR, George AL Jr, and Balser JR (2002) Extracellular sodium interacts with the HERG channel at an outer pore site. *J Gen Physiol* **120:**517–537.

Numaguchi H, Johnson JP Jr, Petersen CI, and Balser JR (2000) A sensitive mechanism for cation modulation of potassium current. *Nat Neurosci* **3:**429–430.

Perry M and Sanguinetti MC (2008) A single amino acid difference between ether-a-go-go-related gene channel subtypes determines differential sensitivity to a small molecule activator. *Mol Pharmacol* **73:**1044–1051.

Polak S, Wiśniowska B, and Brandys J (2009) Collation, assessment and analysis of literature in vitro data on hERG receptor blocking potency for subsequent modeling of drugs' cardiotoxic properties. *J Appl Toxicol* **29:**183–206.

Sanguinetti MC, Jiang C, Curran ME, and Keating MT (1995) A mechanistic link between an inherited and an acquired cardiac arrhythmia: HERG encodes the IKr potassium channel. *Cell* **81:**299–307.

Sanguinetti MC and Jurkiewicz NK (1990) Two components of cardiac delayed rectifier K^+current. Differential sensitivity to block by class III antiarrhythmic agents. *J Gen Physiol* **96:**195–215.

Schönherr R and Heinemann SH (1996) Molecular determinants for activation and inactivation of HERG, a human inward rectifier potassium channel. *J Physiol* **493:**635–642.

Schwarz JR and Bauer CK (2004) Functions of erg K^+channels in excitable cells. *J Cell Mol Med* **8:**22–30.

Trudeau MC, Warmke JW, Ganetzky B, and Robertson GA (1995) HERG, a human inward rectifier in the voltage-gated potassium channel family. *Science* **269:**92–95.

Wang S, Liu S, Morales MJ, Strauss HC, and Rasmusson RL (1997) A quantitative analysis of the activation and inactivation kinetics of HERG expressed in *Xenopus* oocytes. *J Physiol* **502:**45–60.

Warmke JW and Ganetzky B (1994) A family of potassium channel genes related to eag in *Drosophila* and mammals. *Proc Natl Acad Sci USA* **91:**3438–3442.

Weerapura M, Nattel S, Chartier D, Caballero R, and Hébert TE (2002) A comparison of currents carried by HERG, with and without coexpression of MiRP1, and the native rapid delayed rectifier current. Is MiRP1 the missing link? *J Physiol* **540:**15–27.

Witchel HJ, Milnes JT, Mitcheson JS, and Hancox JC (2002) Troubleshooting problems with in vitro screening of drugs for QT interval prolongation using HERG K^+channels expressed in mammalian cell lines and *Xenopus* oocytes. *J Pharmacol Toxicol Methods* **48:**65–80.

Xu X, Recanatini M, Roberti M, and Tseng GN (2008) Probing the binding sites and mechanisms of action of two human ether-a-go-go-related gene channel activators, 1,3-bis-(2-hydroxy-5-trifluoromethyl-phenyl)-urea (NS1643) and 2-[2-(3,4-dichloro-phenyl)-2,3-dihydro-1*H*-isoindol-5-ylamino]-nicotinic acid (PD307243). *Mol Pharmacol* **73:**1709–1721.

Address correspondence to: Christiane K. Bauer, Institut für Zelluläre und Integrative Physiologie, Universitätsklinikum Hamburg-Eppendorf, Martinistraße 52, D-20246 Hamburg, Germany. E-mail: c.bauer@uke.uni-hamburg.de